



Universiteit
Leiden
The Netherlands

TNFalpha-signaling in drug-induced liver injury

Fredriksson, L.E.

Citation

Fredriksson, L. E. (2012, December 6). *TNFalpha-signaling in drug-induced liver injury*. Retrieved from <https://hdl.handle.net/1887/20257>

Version: Corrected Publisher's Version

License: [Licence agreement concerning inclusion of doctoral thesis in the Institutional Repository of the University of Leiden](#)

Downloaded from: <https://hdl.handle.net/1887/20257>

Note: To cite this publication please use the final published version (if applicable).

Cover Page



Universiteit Leiden

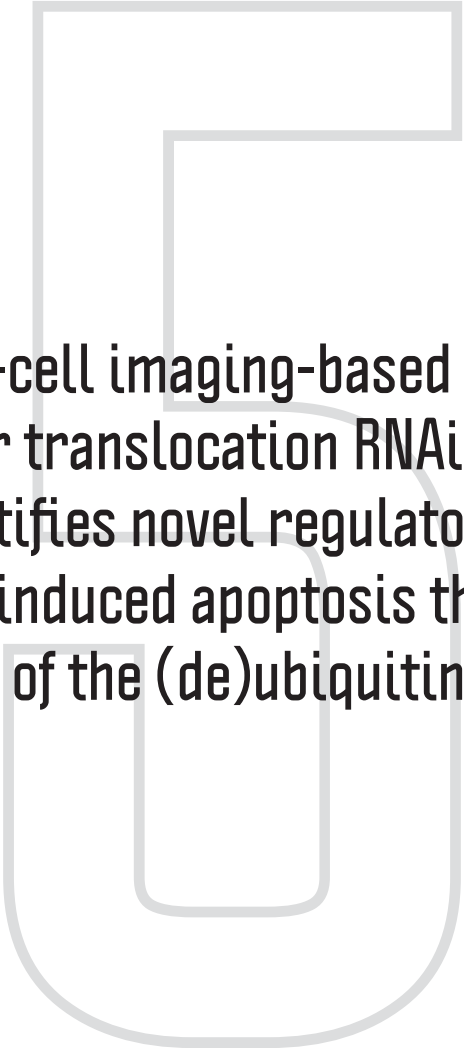


The handle <http://hdl.handle.net/1887/20257> holds various files of this Leiden University dissertation.

Author: Fredriksson, Lisa Emilia

Title: TNFalpha-signaling in drug-induced liver injury

Issue Date: 2012-12-06



**A live-cell imaging-based NF- κ B
nuclear translocation RNAi screen
identifies novel regulators of
TNF α -induced apoptosis through
control of the (de)ubiquitinase A20**

Lisa Fredriksson*, Bram Herpers*, Giulia Benedetti*, Zi Di, Hans de Bont,
John Meerman, Marjo de Graauw and Bob van de Water

Manuscript in preparation

ABSTRACT

Stimulation of cells with the cytokine tumor necrosis factor alpha (TNF α) triggers cytoplasmic-to-nuclear oscillation of the dimeric transcription factor NF- κ B (NF- κ B). In the nucleus, NF- κ B stimulates transcription of its own response inhibitors, I κ B α and the (de)ubiquitinase A20. The concerted induction of I κ B α and A20 functions to prevent over-activation of the response and the time-dependent inactivation is observed as a dampened NF- κ B nuclear oscillation pattern. The number of nuclear oscillations dictates the transcription of downstream pro-inflammatory, anti-oxidant and anti-apoptotic genes. The number of nuclear translocation events is markedly reduced under hepatotoxic drug (diclofenac) exposure conditions in association with enhanced apoptosis. To understand the mechanism of the perturbed oscillatory response, we used a live-cell imaging-based siRNA screen to identify individual kinases, (de)ubiquitinases and sumoylases that control the NF- κ B oscillatory response. We applied high content confocal laser scan microscopy in combination with multiparametric image analysis to follow the NF- κ B oscillation in ~300 individual cells per condition simultaneously. Out of the ~1500 genes screened, we identified 115 that significantly affected the NF- κ B oscillatory response. Using 4 individual siRNAs, we confirmed the action for 46 genes, which affected: (i) the amplitude or duration of nuclear oscillations; (ii) the time between oscillations, leading to an increase or decrease of the number of nuclear translocations; or (iii) an inhibition of the response altogether. In this last category we identified five genes, three novel, whose reduced expression protected against the diclofenac/TNF α -induced apoptosis. Interestingly, the knockdown of four of these genes led to a basic up-regulation of A20 expression. In accordance, A20 knockdown promoted the NF- κ B oscillation and enhanced apoptosis. Double knockdown experiments indicated a direct relationship between these four genes and A20 in the control of the NF- κ B activation. These findings indicate that the (de)ubiquitinase A20 is a master regulator in the life-death decision upon TNF α stimulation in drug-induced hepatotoxic responses, which, in turn, is kept under control by a network of genes that control its expression level.

INTRODUCTION

The dimeric transcription factor nuclear factor- κ B (NF- κ B) controls the expression of a wide array of genes that play an important role in many stages of both physiology and disease. The activity of NF- κ B is crucial in the host-pathogen response by transcribing anti-oxidant and pro-inflammatory genes and thereby activating the innate and adaptive immune response (1). In addition, the activity of NF- κ B has been associated with disease states such as cancer, chronic inflammatory diseases and atherosclerosis (2). The malignant role of NF- κ B arises from improper regulation of its activation. Enhanced activation of NF- κ B leads to over-expression of genes responsible for proliferation, angiogenesis, metastasis, tumor promotion, inflammation and suppression of apoptosis, which gives the transcription factor its tumorigenic properties (3,4). Yet on the other hand, inhibition of NF- κ B activity has been associated to toxicity of drugs (5,6).

NF- κ B is activated by canonical and atypical signaling pathways. The canonical pathway is typically activated by pro-inflammatory stimuli such as the cytokines tumor necrosis factor- α (TNF α) and interleukin-1 β (IL-1 β) that bind to their respective receptors TNFR and IL-1R. Receptor activation is followed by the assembly of a signaling complex composed of several adaptor molecules, ubiquitin ligases and kinases to promote activation of the IKK-complex, the rate-limiting step of NF- κ B pathway signaling. The IKK-complex consists of the catalytic subunits CHUK (IKK α) and IKBKB (IKK β) and the regulatory subunit IKBKG (IKK γ or NEMO) (7). The active IKK complex phosphorylates the inhibitor of NF- κ B, I κ B, which is subsequently poly-ubiquitinated and degraded by the proteasome. This process un masks the nuclear localization signal in NF- κ B, allowing its nuclear translocation and initiation of NF- κ B driven gene transcription (8). De-regulation of the IKK-complex is observed in different cancers, for example through activating mutations in NF- κ B signaling promoting genes such as the NF- κ B inducing kinase (NIK; MAP3K14) or inactivating mutations in NF- κ B signaling repressors such as the deubiquitinase cylindromatosis (CYLD) (9), indicating that NF- κ B activity requires tight regulation to control normal cellular physiology.

To understand this regulatory control, the NF- κ B pathway has been subject to different screening approaches to further decipher its intracellular signaling. Gain- and loss-of-function screens based on NF- κ B luciferase reporter constructs (10,11) were performed using cDNA (10) or RNA-interference (siRNA) screens (11,12). These end-point assay screens focused on the prolonged NF- κ B activity, and were unable to unravel the complex regulatory mechanisms involved in NF- κ B activity that determine the spatial and temporal behavior of NF- κ B after receptor stimulation.

The nuclear translocation of NF- κ B is an oscillatory response that is controlled by feedback control mechanisms and varies between individual cells. Importantly, these NF- κ B oscillations determine the extent and levels of gene transcription (13-15). These oscillatory responses varies within a cell population and is dependent on regulation by post-translational modifications such as phosphorylation, (de)ubiquitination and sumoylation (16). TNF α -induced activation requires K63 and linear (poly-)ubiquitination chains to

allow (auto-)phosphorylation of the IKK kinases to promote K48 linked poly-ubiquitination of I κ B (8). Termination depends on deubiquitination as well as ubiquitination processes, as exemplified by the protein A20 (TNFAIP3). A20 deubiquitinates the activating K63 chains from receptor-interacting protein 1 (RIP1), a TNFR associated kinase upstream of the IKK-complex, and replaces these by K48 chains, marking RIP1 for proteasomal degradation (17,18). As TNFAIP3 and NFKBIA (I κ B α) are two of the principle early target genes of NF- κ B, this provides a very important negative feedback loop to control NF- κ B activation and constitutes the reason for the dampened oscillatory translocation pattern of NF- κ B (19). Also drugs that cause liver failure in patients strongly affect the NF- κ B oscillatory response (5).

In the current manuscript we searched for novel regulatory components of the oscillatory nuclear translocation response of the canonical NF- κ B subunit p65 (RelA) upon exposure to the pro-inflammatory cytokine TNF α . We studied this in the context of drug-induced liver injury responses. By combining RNAi and using live high content confocal imaging of green fluorescent protein tagged p65 (GFP-p65), in a HepG2 cell background, we here present an advanced screening approach to quantitatively determine the effect of individual gene knockdowns on the temporal and spatial behavior of NF- κ B in single cells as well as at the population level. We identified several genes that are essential for the regulation of the A20 protein levels, which thereby not only control NF- κ B oscillation, but also the susceptibility of TNF α -mediated enhancement of drug-induced toxicity.

MATERIALS AND METHODS

Reagents and antibodies

Human recombinant TNF α was acquired from R&D Systems (Abingdon, UK). Diclofenac sodium and the antibody against tubulin were from Sigma-Aldrich (Zwijndrecht, The Netherlands). AnnexinV-Alexa633 and AnnexinV-Alexa561 were made as described (20). The antibody against phospho-specific I κ B α was from Cell Signaling (Bioké, Leiden, The Netherlands). The antibody against A20 was from Santa Cruz (Tebu-Bio, Heerhugowaard, The Netherlands). The bromo phenol blue solution was from Merck (Merck Millipore, Amsterdam Zuidoost, The Netherlands).

Cell culture

Human hepatoma HepG2 cells were obtained from American Type Culture Collection (clone HB-8065, ATCC, Wesel, Germany). HepG2 cells stably expressing GFP-p65 (NF- κ B subunit) were created by 400 μ g/ml G418 selection upon pEGFP-C1-p65 transfection using Lipofectamine™ 2000 (Invitrogen, Breda, Netherlands). HepG2 BAC I κ B α -GFP cells were generated by bacterial artificial chromosome (BAC) recombineering (21,22). Upon validation of correct C-terminal integration of the GFP-cassette by PCR, the BAC-GFP construct was transfected using Lipofectamine™ 2000. Stable HepG2 BAC I κ B α -GFP cells were obtained by 500 μ g/ml G418 selection. For all experiments the cells were cultured in Dulbecco's modified Eagle's medium (DMEM) supplemented with 10%

(v/v) fetal bovine serum (FBS), 25 U/ml penicillin, and 25 μ g/ml streptomycin between passages 5 and 20.

RNA interference

Transient knockdowns of individual target genes were achieved using siGENOME SMARTpool siRNA reagents in the primary screen or single siRNA sequences in the secondary deconvolution screen (50 nM; Dharmacon Thermo Fisher Scientific, Landsmeer, Netherlands). HepG2 cells were transfected using INTERFERin siRNA transfection reagent according to the manufacturer's procedures (Polyplus transfection, Leusden, Netherlands) and left for 72 hours to achieve maximal knockdown before treatment. The negative controls were siGENOME non-targeting pool #1, caspase-8 and mock (INTERFERin only) transfection.

Exposures

Prior to imaging, nuclei were stained with 100 ng/ml Hoechst 33342 in complete DMEM for 45 minutes. The cells were then exposed to Diclofenac 500 μ M or DMSO 0.2% for 8 hours. The cells were then challenged with human TNF α (10 ng/ml).

Live Cell Imaging of GFPp65 and GFP-I κ B α in HepG2 Cells

The GFP-p65 nuclear translocation response and I κ B α -GFP level response upon 10 ng/ml human TNF α challenge was followed for a period of 6 hours by automated confocal imaging every 6 minutes (Nikon TiE2000, Nikon, Amstelveen, Netherlands). Quantification of the nuclear/cytoplasmic ratio of GFPp65 intensity in individual cells was performed using an algorithm for ImageJ (Z. Di, B. Herpers, L. Fredriksson, K. Yan, B. van de Water, F.J. Verbeek and J.H.N. Meerman, submitted).

Translocation response class definition and hit definition

For the primary screen, the amplitudes of the individual translocation response tracks were normalized to their intrinsic response maxima (=1) and minima (=0) to be able to compare the timing of the nuclear translocation events versus the plate average. For the secondary screen, non-normalized data were used. Four different classes were defined according to the type of nuclear p65 oscillation response: increased, no oscillation, decreased and different compared to the oscillation observed with control siRNA. Each class used a different set of five specific parameters (Fig. 1A). For each targeted gene, a Pearson's chi-squared cumulative statistic was calculated from the set of five parameters of each class and p-values were obtained by comparing the value of the statistic to a chi-squared distribution. Targeted genes obtaining a p-value lower than or equal to 0.001 were considered as hits.

Apoptosis measurements

Apoptosis was determined by the live cell apoptosis assay previously described (5,20). The relative Annexin V fluorescence intensity per image was quantified using Image Pro

(Media Cybernetics, Bethesda, MD) and normalized to the number of nuclei or cell area to obtain the estimated percentage of apoptosis.

Western Blot

Cells were harvested in sample buffer (6 times diluted bromo phenol blue solution with β -mercaptoethanol). The samples were subjected to protein separation, blotted on Immobilon-P (Millipore, Amsterdam, The Netherlands). Phosphorylated I κ B α was detected using the Tropix Western-Star kit™ (Applied Biosystems) following manufacturer's protocol. For tubulin and A20, the membranes were blocked for 1 h at room temperature in milk powder 5% (w/v) in Tris-buffered saline/Tween 20 (TBS-T). Primary antibody incubation was done overnight at 4°C followed by incubation with cy5-labeled secondary or horseradish peroxidase-conjugated antibodies (Jackson Immunoresearch, Newmarket, UK) in 1% BSA in TBS-T for 1 h at room temperature. Protein signals were detected with ECL (GE Healthcare) followed by film detection for A20 or by visualization on the Typhoon 9400 imager (GE Healthcare, Diegem, Belgium) for tubulin.

Statistical procedures

All numerical results are expressed as mean \pm standard error of the mean (SEM). Statistical significance was determined by GraphPad Prism using an unpaired t-test, * $P \leq 0.05$, ** $P \leq 0.01$, *** $P \leq 0.001$. Heatmap representations and hierarchical clustering (using Pearson correlation) were performed using the MultiArray Viewer software.

RESULTS

NF- κ B nuclear oscillation phenotype siRNA screening in HepG2 cells

Stimulation of cells with TNF α initiates nuclear translocation oscillation of the NF- κ B transcription factor. To follow the dynamics of this process, we created a stable GFP-tagged HepG2 reporter line for the NF- κ B subunit p65/RelA. Time-lapse confocal microscopy showed that the nuclear translocation of GFP-p65 is transient and follows a dampened oscillation at set time intervals, largely due to NF- κ B-dependent transcription of I κ B α (19). Under control conditions, the initial translocation peaks at 30 minutes after TNF α (10 ng/mL) stimulation, followed by a second and third peak at 120 minute intervals (Figure 1 A, top). In HepG2 cells this effect was maximal at 10 ng/mL (data not shown). Successful knockdown with siRNAs targeting A20 (Supporting Data S1) slightly decreased the time-interval between oscillations, leading to faster oscillation, whereas knockdown of I κ B α (Supporting Data S1) almost completely inhibits NF- κ B oscillation in association with enhanced levels of p65-GFP expression (Fig. 1 A, middle). Pre-incubation of HepG2 cells with 500 μ M diclofenac for 8 hours increased the time interval between peaks (Fig. 1 A, bottom; (5)). To distinguish these four phenotypes (control, increased oscillation, decreased oscillation and no oscillation) from each another, we established a pipeline of automated image segmentation and GFP-p65 nuclear/cytoplasmic ratio quantification for

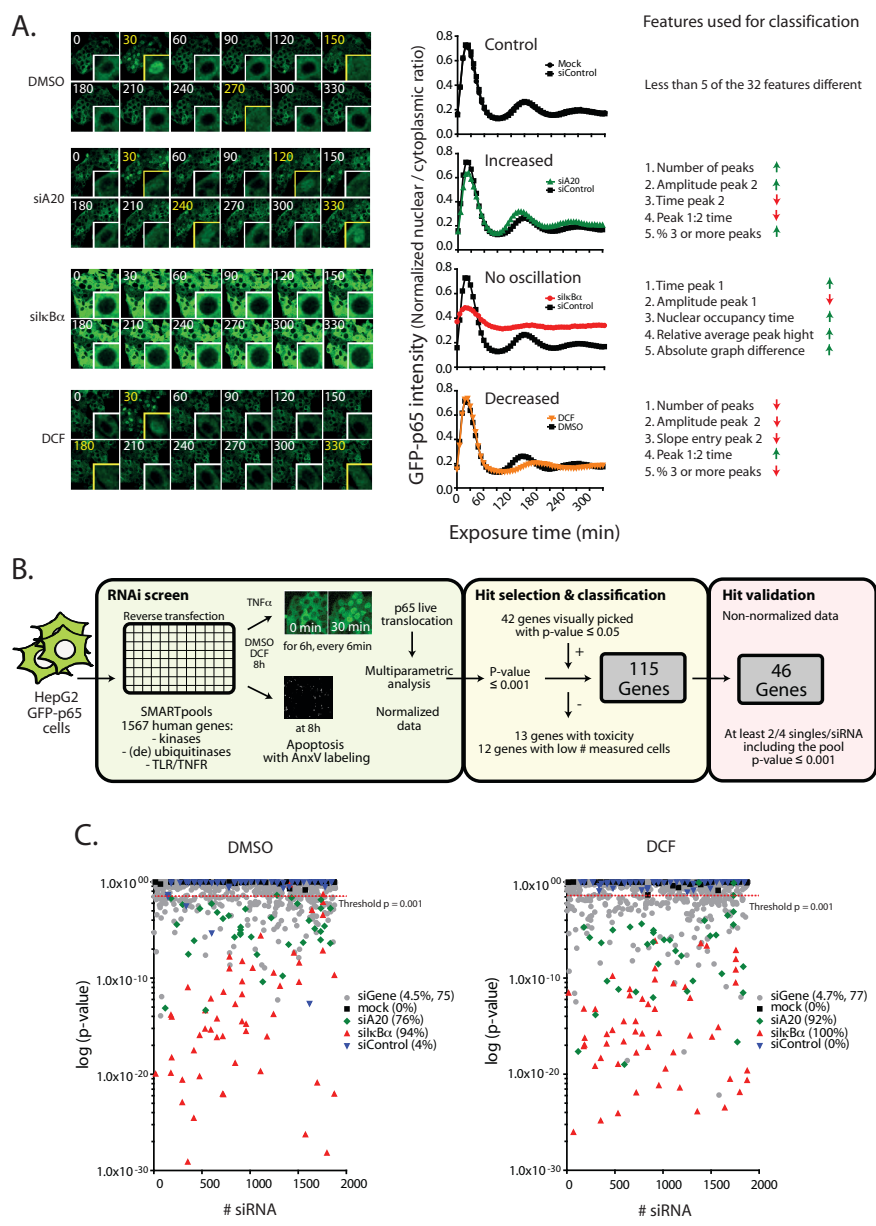


Figure 1. *NF- κ B* oscillation phenotype siRNA screening in HepG2 cells. (A) Representative images of GFP-p65 translocation after TNF α (10 ng/mL) challenge in HepG2 cells by automated confocal microscopy. Insets: zooms of single cells with an average response in respect to the imaged population. The nuclear translocation events are marked by yellow boxes and the numbers indicate the time in minutes after TNF α exposure. The nuclear translocation track of each cell was quantified and normalized to its own highest nuclear-to-cytoplasmic ratio (value of 1) and its lowest ratio (0). The average response of the total cell population is presented in the middle panel. The features and their directions that define the response classes (different, increased, decreased and no oscillation) compared to control are shown in the panel to the right. (B) Flowchart of the siRNA screen. (C) P-value distribution of the hits and the positive and negative controls. Under DMSO conditions the true discovery rate was 0.94 and 0.76 for silkBx and siA20 respectively while the false discovery rate was 0.04. Under DCF conditions the corresponding values were, 1, 0.92 and 0 respectively. 4.5% of the screened genes were found to have an effect on the oscillation under DMSO conditions while 4.7% were determined to give a significant effect after DCF pre-exposure.

all individual cells within one time-series, followed by extraction of 32 distinct oscillation features (Di *et al.*, submitted). We classified the phenotypes based on the direction versus control for at least five oscillation features, e.g. number of peaks, time between peaks and amplitude of peaks (Fig. 1 A). If more than 5 of the 32 measured oscillation features were distinct from control and the oscillation phenotype did not match any of the other categories, the response was marked as “different oscillation”.

Having established an automated system to track, segment and categorize the NF- κ B oscillation pattern in individual cells, we set out to identify the genes that are responsible for the timely activity of the NF- κ B response by siRNA screening (Figure 1 B). We screened 779 kinases, 107 de-ubiquitinases and sumoylases, 580 ubiquitin ligases and 123 pre-described players in the TNFR/TLR-driven NF- κ B response, under DMSO (control) and diclofenac (DCF) conditions. 22 siRNAs were overlapping in either of the libraries. Annexin-V-Alexa633 labeling of the cells allowed us to omit the genes that induce apoptosis upon knockdown. For all target genes the oscillation of the GFP-p65 reporter was followed for 6 hours at 6 minute intervals, directly after TNF α stimulation. Because we were mainly interested in the time between oscillations under control and DCF conditions, we normalized the nuclear/cytoplasmic GFP intensity ratio and separated the analysis for both conditions. Within each condition, we considered genes a potential hit at a p-value below or equal to 0.001, a minimum of in total 35 cells analyzed (average number of cells was 184 per condition) and absence of apoptosis. Within this p-value cut-off we could trace back the effect of A20 knockdown under control and DCF conditions in 76% and 92% of the samples, respectively; and the effect of I κ B α knockdown in 94% and 100% of the samples (Fig. 1 C). Another 42 genes were added from the “different” category, based on visual inspection of the translocation phenotype and taking the p-value into consideration ($P \leq 0.05$). In total we re-screened 115 genes by using 4 single siRNAs targeting the same gene, of which 46 genes were confirmed to affect the GFP-p65 oscillation with 2 or more single siRNAs in addition to the pooled siRNAs in either or both DMSO and DCF conditions.

Functional and phenotypic classification of the siRNA screen hits that control NF- κ B oscillation

Out of the 46 confirmed hits, 5 genes, including the known inhibitor of NF- κ B activation, UCHL1 (23), decreased the oscillation after knockdown; 7 increased the oscillation, also confirming the inhibitory role for TNFAIP3 (A20) for the activation of NF- κ B; 24 showed no oscillation, including the essential activators of NF- κ B I κ BKG (IKK γ) and ubiquitin ligase CUL1, needed for the polyubiquitination of I κ B α (24), and 4 did not fall in the previous three categories, but were significantly different from the controls under DMSO conditions (Figure 2 A-B and Table 1). Despite the oscillation-decreasing effect of DCF, 2 siRNAs targeting splicing factor PHF5A and th receptor TNFRSF18, led to a further decrease in oscillation under this condition. Twelve increased the oscillation, 22 stopped the oscillation, including knockdown of the cyclin-dependent kinase CDK12 that was

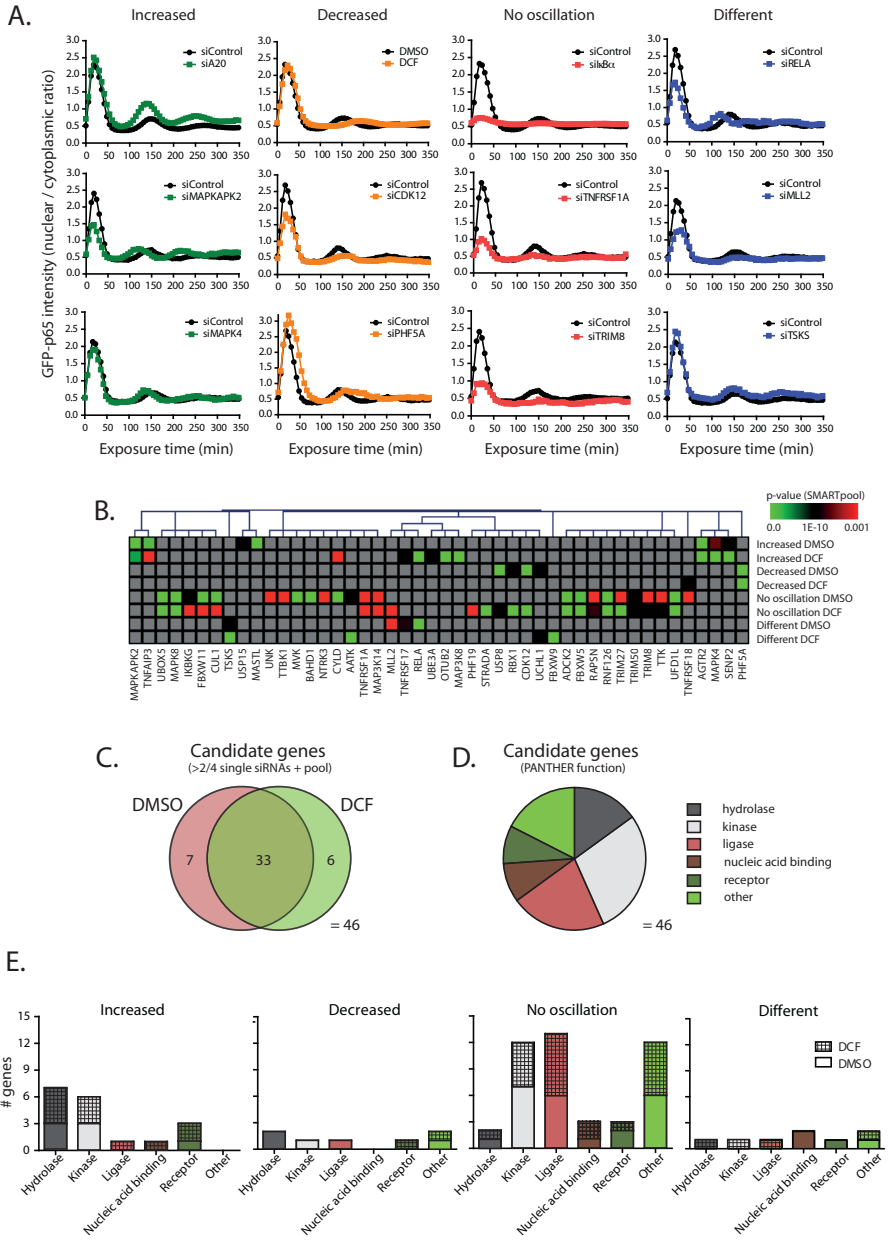


Figure 2. Functional and phenotypic profiling of the siRNA screen hits that control NF- κ B oscillation. (A) Typical non-normalized NF- κ B oscillation averages acquired in the deconvolution screen, including examples of knockdowns that led to a phenotype similar to the classification controls; siA20, diclofenac (DCF) and si κ B α . The “different” class is defined by having five or more features significantly different from the siControl. (B) Heatmap of the SMARTpool classification P-values for the hits confirmed by 2 or more single siRNAs in the deconvolution screen, clustered for their corresponding classification on the right. The overlap of the hits under DMSO and DCF conditions are additionally presented in (C). (D) Most of the hits under both DMSO and DCF conditions are described as kinases, (ubiquitin) ligases and hydrolases (mostly deubiquitinases). (E) Knockdown of hydrolases led to a predominantly “increased” phenotype under both DMSO and DCF conditions, while knockdown of kinases and ligases in general lead to “no oscillation” phenotype. The “decreased” phenotype was predominantly detectable under DMSO conditions. The functionality of the target genes was evenly distributed. The “different” phenotype was evenly distributed over functionality as well as exposure condition.

Table 1. Confirmed hits from the deconvolution screen arranged by classification. DCF = diclofenac.

| Gene Symbol | Name (also known as) | Function | DMSO | DCF | # singles DMSO | # singles DCF | Regulator of NF- κ B | Reference |
|-----------------------|---|-------------------------------|-------------------|-------------------|----------------|---------------|-----------------------------|------------|
| PHF5A | PHD finger protein 5A | splicing factor hydrolyase | Decreased | Decreased | 4/4 | 3/4 | (-) | (1) |
| UCHL1 | ubiquitin carboxyl-terminal esterase L1 | | Decreased | Different pattern | 2/4 | 4/4 | | |
| AGTR2 | angiotensin II receptor type 2 (AT2) | receptor | Increased | Increased | 3/4 | 3/4 | Activator/Inhibitor | (2,3) |
| MAPK4 | mitogen-activated protein kinase 4 (ERK-4) | kinase | Increased | Increased | 3/4 | 2/4 | (-) | (4) |
| MAPKAPK2 | mitogen-activated protein kinase-activated protein kinase 2 (MK2) | kinase | Increased | Increased | 2/4 | 2/4 | Inhibitor | (5,6) |
| SEN2 | SUMO1/sentrin/SMT3 specific peptidase 2 | hydrolyase | Increased | Increased | 2/4 | 4/4 | Inhibitor/Activator | (7) |
| TNFAIP3 | tumor necrosis factor alpha-induced protein 3 (A20) | hydrolyase/ligase | Increased | Increased | 2/4 | 3/4 | Inhibitor | (8) |
| RELA | v-rel reticuloendotheliosis viral oncogene homolog A (p65) | nucleic acid binding | Different pattern | Increased | 3/4 | 4/4 | Inhibitor | (9,10) |
| TNFRSF17 | tumor necrosis factor receptor superfamily member 17 (BCMA) | receptor | Different pattern | Increased | 3/4 | 3/4 | Activator | |
| No oscillation | | | | | | | | |
| CDK12 | cyclin-dependent kinase-12 (CRK2, CtrA85) | kinase | Decreased | No oscillation | 3/4 | 3/4 | (-) | (11,12) |
| RBX1 | ring-box 1 | ligase | Decreased | No oscillation | 2/4 | 2/4 | Inhibitor | |
| USP8 | ubiquitin specific peptidase 8 | hydrolyase | Decreased | No oscillation | 2/4 | 3/4 | (-) | (13) |
| TNFRSF18 | tumor necrosis factor receptor superfamily member 18 (GITR) | receptor | No oscillation | Decreased | 4/4 | 3/4 | Activator | |
| ADCY2 | adenylyl cyclase 2 | unclear | No oscillation | No oscillation | 4/4 | 2/4 | (-) | (14) |
| CUL1 | culin 1 | ligase | No oscillation | No oscillation | 3/4 | 3/4 | Activator | (15) |
| FBXW11 | F-box and WD repeat domain containing 11 (BTRCP2) | ligase | No oscillation | No oscillation | 4/4 | 4/4 | Activator | (16) |
| FBXW5 | F-box and WD repeat domain containing 5 | ligase | No oscillation | No oscillation | 3/4 | 2/4 | Inhibitor | (17) |
| IKBKG | inhibitor of kappa light polypeptide gene enhancer in B-cells kinase gamma (NEMO) | enzyme regulator | No oscillation | No oscillation | 4/4 | 4/4 | Activator | (18) |
| MAP3K14 | mitogen-activated protein kinase kinase kinase 14 (NIK) | kinase | No oscillation | No oscillation | 2/4 | 2/4 | Activator | (19) |
| MAPK8 | mitogen-activated protein kinase 8 (JNK1) | kinase | No oscillation | No oscillation | 4/4 | 3/4 | Inhibitor | |
| RAPSN | receptor-associated protein of the synapse (lapsyn) | receptor adaptor protein | No oscillation | No oscillation | 3/4 | 3/4 | (-) | (8) |
| RNF126 | ring finger protein 126 | unclear | No oscillation | No oscillation | 3/4 | 3/4 | (-) | (20) |
| TNFRSF1A | tumor necrosis factor receptor superfamily member 1A (TNFR1) | receptor | No oscillation | No oscillation | 4/4 | 4/4 | Activator | |
| TRIM27 | tripartite motif containing 27 (RFP) | ligase | No oscillation | No oscillation | 3/4 | 2/4 | Inhibitor | |
| TRIM50 | tripartite motif containing 50 | ligase | No oscillation | No oscillation | 3/4 | 2/4 | (-) | (21,22,23) |
| TRIM8 | tripartite motif containing 8 | ligase | No oscillation | No oscillation | 2/4 | 2/4 | (-) | |
| TTK | TTK protein kinase (PYT) | kinase | No oscillation | No oscillation | 3/4 | 3/4 | Activator | |
| UBOX5 | U-box domain containing 5 | enzyme modulator | No oscillation | No oscillation | 3/4 | 3/4 | (-) | |
| UBFD1L | ubiquitin fusion degradation 1 like | enzyme modulator | No oscillation | No oscillation | 4/4 | 3/4 | (-) | |
| Miscellaneous | | | | | | | | |
| TSKS | testis-specific serine kinase substrate | unclear | Different pattern | Different pattern | 3/4 | 2/4 | (-) | |
| NLL2 | myeloid/lymphoid or mixed-lineage leukemia 2 | nucleic acid binding | Different pattern | No oscillation | 3/4 | 2/4 | (-) | |
| AATK | apoptosis-associated tyrosine kinase (AATYK) | kinase | No oscillation | Different pattern | 4/4 | 3/4 | (-) | |
| CYLD | cylindromatosis | hydrolyase | No oscillation | Increased | 4/4 | 2/4 | Inhibitor | (24) |
| NTRK3 | neurotrophic tyrosine kinase receptor type 3 (TRKC) | kinase | No oscillation | not different | 3/4 | (-) | (-) | |
| BAHD1 | bromo adjacent homology domain containing 1 | nucleic acid binding | No oscillation | not different | 3/4 | (-) | (-) | |
| MVK | mevalonate kinase | kinase | No oscillation | not different | 3/4 | (-) | (-) | |
| TUBK1 | tau tubulin kinase 1 | kinase | No oscillation | not different | 3/4 | (-) | (-) | |
| UNK | unkempt homolog (unkempt) | ligase | No oscillation | not different | 3/4 | (-) | (-) | |
| FBXW9 | F-box and WD repeat domain containing 9 | ligase | not different | Different pattern | (-) | 3/4 | (-) | |
| MAP3K8 | mitogen-activated protein kinase kinase kinase 8 (COT; TPL2) | kinase | not different | Increased | (-) | 2/4 | Activator | (25) |
| OTUB2 | OTU domain ubiquitin aldehyde binding 2 | hydrolyase | not different | Increased | (-) | 2/4 | Inhibitor | (26,27) |
| UBE3A | ubiquitin protein ligase E3A | ligase | not different | Increased | (-) | 2/4 | (-) | |
| PHF19 | PHD finger protein 19 | nucleic acid binding | not different | No oscillation | (-) | 3/4 | (-) | |
| STRADA | STE20-related kinase adaptor alpha (STRADA/alpha) | kinase | not different | No oscillation | (-) | 2/4 | (-) | |
| MAS1L | microtubule associated serine/threonine kinase like (greatwall) | kinase | Increased | not different | 2/4 | (-) | (-) | |
| USP15 | ubiquitin specific peptidase 15 | hydrolyase | Increased | not different | 3/4 | (-) | Inhibitor | (28) |

shown to only decrease the oscillation under DMSO conditions, and 4 had a different oscillation phenotype (Fig. 2 B and Table 1). Between the two conditions, 33 hits were overlapping, 7 were unique for DMSO and 6 for the diclofenac condition at a p-value cut-off of $p < 0.001$ (Fig. 2 B-C and Table 1). Most hits were kinases and (ubiquitin) ligases, which most often contributed to the “no oscillation” or “decreased” response phenotype (Fig. 2 D and 2 E).

The strength of our siRNA screening approach is the analysis of the dynamics of the NF- κ B response at the single cell level within an entire population of cells. This allows measurement of the population dynamics upon knockdown of our candidate genes (Fig. 3 A and 3 B). Under control conditions the majority of the cells showed three nuclear translocation events within the imaging period. Yet the siRNA conditions that blocked the oscillation led to profiles with either no, or one shallow oscillation event, as shown with our positive control I κ B α and knockdown of the genes necessary for NF- κ B activation, IKBKG (IKK γ) and TNFRSF1A (TNFR1) (Fig. 3 Bi). The decreased phenotype exhibited mainly 2 or 3 oscillation events, as shown by knockdown of CDK12 and PHF5A, whereas the increased class, best illustrated by knockdown of our positive control TNFAIP3 (A20), showed mostly cells with 3 or 4 oscillations (Fig. 3 Bii). Within the profile class of “no oscillation” the number of peaks was vastly reduced and any observable translocation event occurred later than in control cells, at lower amplitude and with a reduced nuclear entry slope. Within the remaining fraction of cells (~30%) that showed more than one nuclear translocation event, the peaks remained shallow, which leads to a reduced dampening between the peaks (Fig. 3 Ci). The group of siRNAs that decreased the oscillation also decreased the number of oscillations and increased the time of the first translocation event. Differently from the “no oscillation” class, the profiles within the “decreased” class that included CDK12, RBX1, PHF5A and USP8, all showed an increase in the duration of the initial translocation event including a delayed time for the maximum. This suggests a role in the regulation of the NF- κ B nuclear export, which subsequently affects the timing of the second peak (Figure 3 Cii). Finally, the increased class, including our positive control TNFAIP3 (A20), the inhibitor of NF- κ B activation MAPKAPK2 (25), AGTR2 and MAPK4, were hallmarked by an increase in the number of oscillations, with a decreased time interval between peaks, that exhibit an elevated NF- κ B nuclear translocation amplitude (Figure 3 Ciii).

Genes that prevent the NF- κ B oscillation protect against TNF α /hepatotoxicant-induced cell death.

Diclofenac (DCF) and carbamazepine (CBZ) are two drugs that are associated with idiosyncratic liver injury in humans, in which the innate immune system-based TNF α is an important component. Indeed, we have previously reported that diclofenac sensitizes liver cells to apoptosis caused by an otherwise non-toxic dose of TNF α (5). Since this was directly linked to inhibition of NF- κ B signaling (5), we questioned whether inhibition of the 22 candidate genes that showed a “no oscillation” phenotype after knockdown,

would affect the cytotoxic response upon DCF/TNF α and CBZ/TNF α exposure. Since knockdown of caspase-8 completely inhibited the apoptotic response induced by both DCF/TNF α and CBZ/TNF α , we further used this as a positive control (Fig. 4 A and B). The majority of the knockdowns that displayed a “no oscillation” phenotype significantly inhibited the drug/TNF α -induced apoptotic response (12 out of 21; including CDK12,

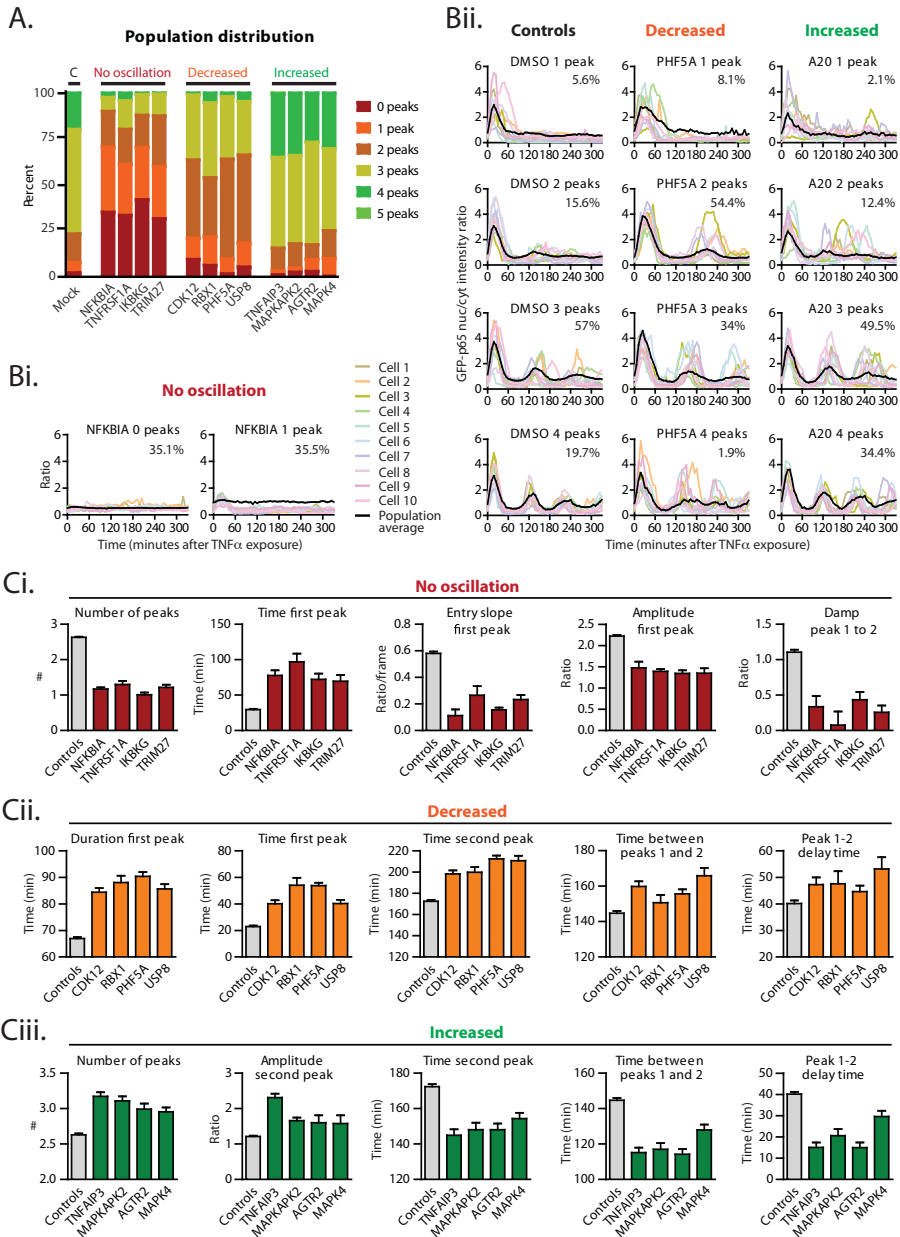


Figure 3. Population statistics. (A) The population distribution of NF- κ B oscillations in HepG2 GFPp65 cells upon indicated siRNA treatments. (B) Examples of how each phenotypic class is distributed in relation to the number of translocation peaks. (C) The translocation features that define the different classes: “no oscillation” (Ci), “decreased” (Cii) and “increased” (Ciii) are exemplified by their representative siRNAs.

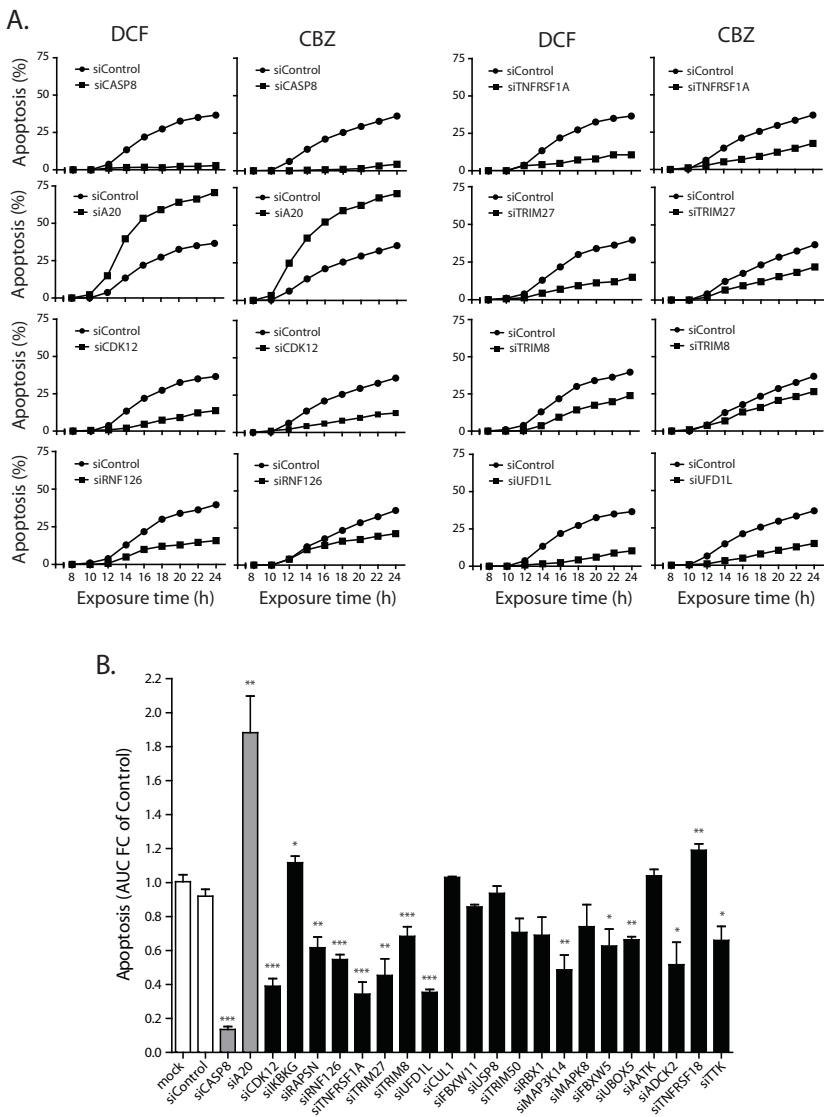


Figure 4. A “no oscillation” phenotype correlates to decreased drug/TNF α -induced apoptosis. (A) Live apoptosis imaging of wild type HepG2 cells with knockdowns resulting in a “no oscillation” phenotype in GFP-p65 cells after 500 μ M diclofenac (DCF) or 500 μ M carbamazepine (CBZ) pre-incubation for 8 hours followed by addition of TNF α (10 ng/mL). The amount of apoptosis is presented as a percentage after normalization to the number of Hoechst33342-positive cells. (B) The area under the curves (AUC) depicted in A was calculated and an average of the fold change (FC) compared to siControl for three independent experiments was determined. The difference in FC AUC compared to siControl was defined using Student’s t-test where * $P \leq 0.05$, ** $P \leq 0.01$ and *** $P \leq 0.001$.

RNF126 and TNFRSF1A), while others did not significantly affect the response (7 out of 21; including CUL1, USP8 and AATK); only IKBKG (IKK γ) and TNFRSF18 knockdowns slightly, but significantly, increased the sensitivity towards apoptosis (Fig. 4 B). Interestingly, knockdown of the important negative regulator of TNF α -induced apoptosis, A20, strongly enhanced the apoptotic response (Fig. 4 A and B).

Protection against apoptosis is correlated to A20 expression and not I κ B α activation

I κ B α is a direct phosphorylation target for the IKK complex after TNF receptor activation and subsequently targeted for proteasomal degradation, a prerequisite for NF- κ B nuclear translocation. In addition, I κ B α constitutes the earliest induced negative feedback mechanism for the attenuation of NF- κ B activity. We wondered whether genes showing the most significant reduction in drug/TNF α -induced apoptosis (p-value < 0.001 in Figure 4B: including CDK12, RNF126, TNFRSF1A, TRIM8 and UFD1L) would affect I κ B α levels. We used BAC-NFKBIA-GFP (I κ B α -GFP) HepG2 cells that phosphorylate and degrade I κ B α -GFP with the same kinetics as non-tagged I κ B α (Supporting Data S2). We knocked down above genes individually and followed the I κ B α -GFP levels by live cell imaging. Depletion of the TNFRSF1A, UFD1L, and RNF126 strongly increased the initial levels of I κ B α -GFP compared to mock treatment (Fig. 5 A), which was associated

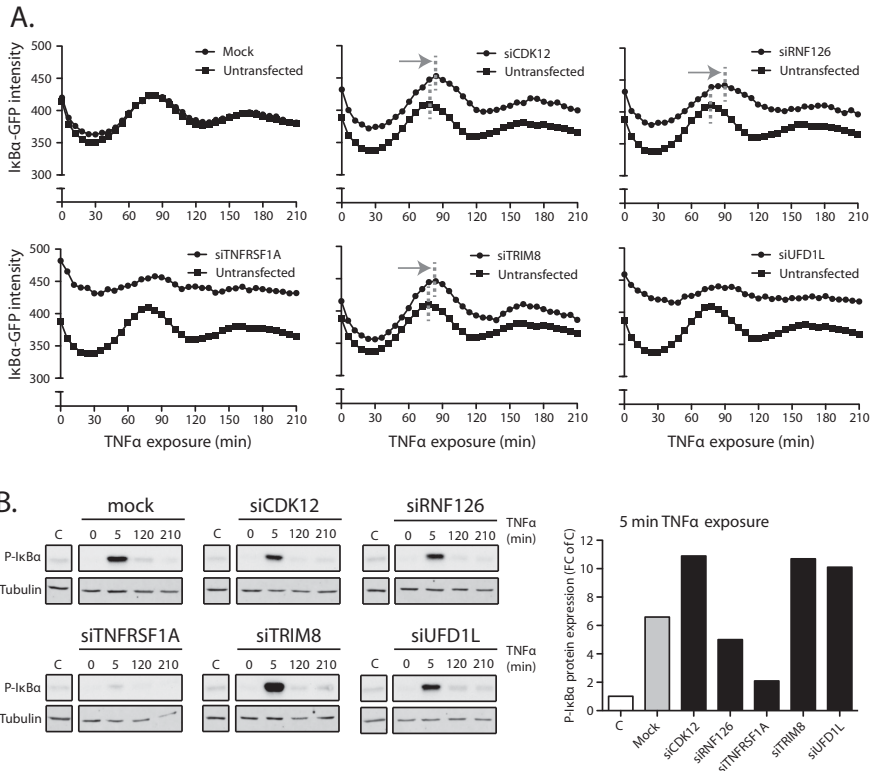


Figure 5. I κ B α levels are elevated and the re-expression is delayed while phosphorylation status remains the same after knockdown of the candidate genes. (A) Quantification of GFP expression in HepG2 cells expressing a BAC-NFKBIA-GFP construct. TNF α stimulation induces degradation and re-synthesis of the I κ B α -GFP protein, which is altered after knockdown of the indicated candidate genes. (B) The amount of I κ B α phosphorylation (P) after knockdown of the indicated candidate genes in HepG2 GFP-p65 cells followed by TNF α exposure for 0, 5, 120 and 210 minutes was determined by western blotting. The tubulin-normalized intensities of P-I κ B α for the same knockdowns after 5 minutes of TNF α exposure is shown in the right panel.

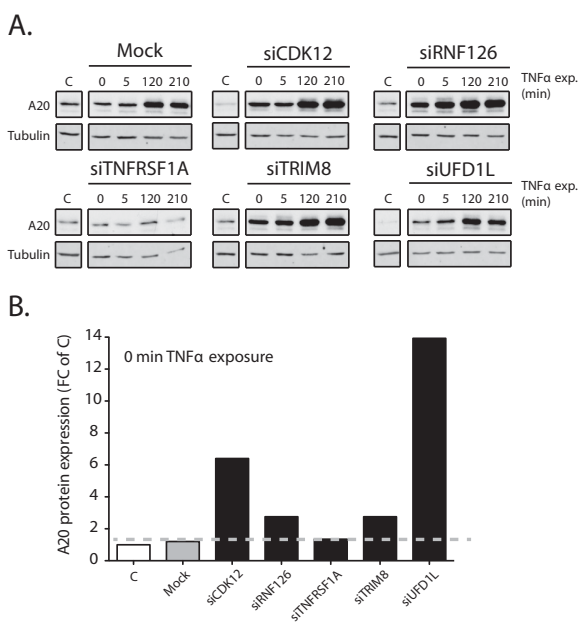


Figure 6. Knockdown of the candidate genes leads to basic upregulation of (de) ubiquitinase A20. (A) Western blot for the A20 expression levels after knockdown of the indicated candidate genes in HepG2 GFP-p65 cells exposed to 10ng/ml TNF α for 0, 5, 120 and 210 minutes. (B) Quantification of the A20 protein levels at time-point 0 in A.

with an essential complete inhibition of the NF- κ B translocation response (see Fig. 2 B). Importantly, TNF α treatment caused an oscillatory response of I κ B α -GFP at the population level, corresponding to the western blot data. As expected, depletion of the TNF receptor inhibited an I κ B α -GFP oscillatory expression. Yet, CDK12, TRIM8 and RNF126 did not affect the initial breakdown of I κ B α -GFP, but slightly delayed the newly translated I κ B α -GFP. In line with this CDK12, TRIM8 and RNF126 did not inhibit the early phosphorylation of I κ B α upon TNF α stimulation; as expected, TNFRSF1A knockdown prevented this phosphorylation event (Fig. 5 B). Knockdown of UFD1L showed a different response: despite the fact that TNF α could initiate a phosphorylation of I κ B α , the degradation of I κ B α -GFP was reduced, suggesting a role for UFD1L in the degradation of this protein (Fig. 5 A and B).

As differences in I κ B α phosphorylation and breakdown were not the major contributors to the effect of CDK12, RNF126, TRIM8 and UFD1L, we turned our attention to a second important negative feedback mechanism for NF- κ B activity, A20 (TNFAIP3) (17,18). Intriguingly, the A20 levels after knockdown of CDK12, RNF126, TRIM8 or UFD1L were increased at control situation, prior to TNF α treatment (Fig. 6 A and B). Regardless, TNF α was still capable to further induce A20 after TNF α exposure (Fig. 6 A) most likely since the first NF- κ B nuclear entry peak is not affected by these knockdowns. Again, as expected, depletion of the TNF α -receptor (TNFRSF1A) did not affect A20 levels under control or TNF α treatment.

A20 was an important regulator of the oscillatory NF- κ B response in HepG2 cells. The above data suggested that the effects of CDK12, RNF126, TRIM8 and UFD1L depletion on the reduced NF- κ B oscillation was a direct result of the increased A20 levels. Therefore, we performed double knockdown experiments by combining A20 siRNAs with the siRNA against CDK12, RNF126, TRIM8 or UFD1L, again using TNFRSF1A as a

positive control. Importantly, depletion of TNF receptor together with A20 did not induce any oscillatory response, indicative for the effectiveness of our double knockdown. Yet, simultaneous knockdown of A20 with either CDK12, RNF126, UFD1L or TRIM8, (partially) recovered the NF- κ B oscillatory response (Fig. 7 A), which was further quantified with respect to the average number of nuclear entry peaks at the cell population level (Fig. 7 B).

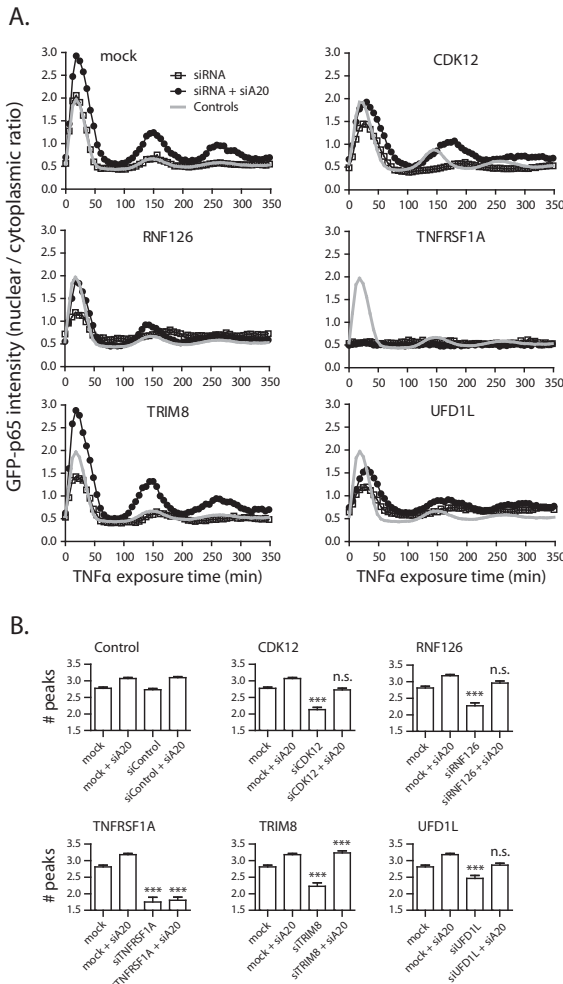


Figure 7. Double knockdown with candidate genes and siA20 leads to restoration of the translocation response. (A) The average oscillatory response in HepG2 GFP-p65 cells upon TNF α addition under double candidate gene and A20 knockdown conditions. Increased oscillation could be observed compared to knockdown of the candidate genes alone. (B) Quantification of the average number of peaks with and without A20 double knockdown. The data represent the average of 3 independent experiments \pm S.E.M. The difference in the number of peaks compared to mock was defined using Student's t-test where *** P \leq 0.001.

DISCUSSION

The transcription factor NF- κ B is an important player in both physiology and disease, and its (enhanced) activity has been implicated in cancer as well as chronic inflammatory diseases (2). In addition, inhibition of NF- κ B signaling has been implicated in the toxicity of drugs (5). The NF- κ B translocation response is tightly controlled by different types of posttranslational modifications such as phosphorylation and especially (de)ubiquitination,

which has received much attention in recent years (16,17). In the current manuscript we have investigated the role of individual kinases, (de)ubiquitinases and sumoylases in the nuclear translocation of the transcription factor NF- κ B following TNF α stimulation using siRNA-mediated knockdowns. For accuracy to determine the dynamics of the response, we employed a high content imaging method including a recently developed image analysis technique to quantify 32 different parameters describing the NF- κ B oscillatory response. Using at least 5 of these features we could distinguish and classify siRNA knockdowns that result in a “no oscillation”, “decreased”, “increased” and significantly “different” translocation phenotype. An siRNA deconvolution screen confirmed 46 of the 115 hits from the primary screen of which the majority showed a “no oscillation” phenotype, and are thus likely to be positive regulators of NF- κ B oscillation (Fig. 2). Many of these positive regulators also control the apoptotic outcome after hepatotoxicant/TNF α -exposure, by regulating the expression levels of the (de)ubiquitinase A20.

We successfully applied an advanced high content imaging approach to identify novel regulators of NF- κ B signaling. So far RNA interference screens for NF- κ B signaling mainly involved endpoint assays that mimic NF- κ B transcriptional activity using luciferase reporter assays (11,12), precluding mechanistic insight in the dynamics of the NF- κ B activation response. Our method allowed us to identify candidate genes that regulate the oscillatory response of NF- κ B. Some of the 46 candidate genes have already been implicated in the regulation of NF- κ B signaling (Table 1). This overlap was primarily observed in the target genes that upon knockdown increased or inhibited an NF- κ B oscillatory response: genes with an “increased” phenotype were previously described as inhibitors of the NF- κ B signaling response, and genes with “no oscillation” phenotypes are associated with promoters of NF- κ B signaling (Table 1).

There is increasing evidence for a role of the oscillatory response of NF- κ B in the control of gene expression. The total duration of nuclear localization and promoter association is likely to define the spatiotemporal control of epigenetic modulation of genes, and thereby their expression. Indeed, the differential expression of early, mid and late NF- κ B target genes seems proportional to the strength and duration of the NF- κ B nuclear occupancy (14,15). I κ B α and A20 are classical early NF- κ B target genes that are also regulated tightly in our model systems and provide early feedback control of NF- κ B activation. At this point we do not know whether our candidate genes that affect the oscillatory response of NF- κ B will also affect the overall target gene expression. We anticipate that such a dynamic transcriptional activity of NF- κ B is likely to differ within the cell population. Indeed, we observed a differential response of the NF- κ B oscillation in our cell population, with around 80% of the cells demonstrating 3 to 4 oscillations in control situations, and only 10% demonstrating one single peak. Depletion of for example TRIM27 completely shifted this response with 80% showing either 0 or 1 oscillation peak. Reversely, MAPKAPK2, AGTR2 and MAPK4 increased the percentage of cells with 4 peaks. These effects will likely determine NF- κ B mediated gene transcription.

Various novel candidates that regulate NF- κ B signaling were identified. We described the splicing factor PHF5A as a promoter of the NF- κ B oscillatory response.

PHF5A is implicated in processing of pre-mRNA (26). We suggest that this gene is required for proper processing of the mRNA of the protein needed for nuclear export of NF- κ B, i.e. I κ B α , after transcriptional activation. Furthermore we implicated the atypical mitogen activated protein kinase (MAPK) 4 (also known as ERK4), in the attenuation of the NF- κ B signaling, since knockdown of this protein resulted in an “increased” translocation phenotype. ERK4 acts as a kinase for the substrate MAPKAPK5 (MK5) (27). We identified MAPKAPK2 (MK2), another protein in the same family as MK5 as an inhibitor of NF- κ B translocation. MK2 is known to inhibit the nuclear export of NF- κ B by reducing the levels of I κ B α (25). MK5 has a similar role as MK2 and both phosphorylate HSP27 (28). Interestingly, HSP27 was previously implicated in the regulation of IKK activity as well as I κ B α function (25,29,30). More research is required to investigate this link.

Previously we reported that inhibition of the NF- κ B translocation is linked to enhanced cytotoxicity following exposure to the hepatotoxicant diclofenac in combination with TNF α (5). Therefore, we focused on the knockdowns that resulted in a “no oscillation” phenotype. As expected, knockdown of known activators of the NF- κ B signaling response, such as IKBKG (IKK γ ; NEMO) and TNFRSF18 (GITR) (Table 1) enhanced the apoptotic response under diclofenac/TNF α and carbamazepine/TNF α exposure conditions (Fig. 4). In addition, knockdown of known inhibitors of the NF- κ B response such as FBXW5 and TRIM27 (RFP) as well as the TNF receptor itself (TNFRSF1A) (Table 1) reduced the apoptotic response (Fig. 4). However, surprisingly, most of the knockdowns that lead to a reduced or no oscillatory response, reduced the drug/TNF α -induced apoptosis, including the known activators of NF- κ B signaling, MAP3K14 (NIK) and TRIM8. Here we report for the first time that this observation is most likely due to the basal induction of the (de) ubiquitinase A20. Higher A20 levels at the start of TNF α exposure would indeed reduce the induction of NF- κ B translocation, as A20 is the most important negative regulator of RIP1 activity (17,18). Furthermore, since A20 also controls apoptosis by deubiquitinating caspase-8 to reduce the activation of this protease (31), the elevated A20 levels might provide cellular protection against drug/TNF α -induced cell death. To our knowledge none of the candidate genes have been previously reported to affect A20 expression.

Since both I κ B α as well as A20 levels were enhanced under control conditions (Fig. 5 A and 6), and both are important target genes of NF- κ B, it seems likely that the enhanced expression of these proteins results from some initial activity of p65 after knockdown of the candidate genes. Especially in UFD1L knockdowns, the A20 and I κ B α levels were exceptionally high. UFD1L is described as part of a complex regulating the proteasomal degradation of polyubiquitinated proteins from the endoplasmic reticulum and implicated in the closure of the nuclear envelope (32). Potentially, lack of UFD1L dismantles the boundary between inactive (cytoplasmic) and active (nuclear) p65, allowing a rise in nuclear p65 presence and thereby transcription of the negative feedback genes A20 and I κ B α , an effect similar to I κ B α knockdown itself (Supporting Data S1). In addition, the higher expression of A20 together with potential upregulation of NF- κ B transcribed anti-apoptotic genes could result in the decreased apoptotic response

observed.

To our knowledge nothing is known about the functions and substrates of the E3 ubiquitin ligase RNF126. However, as discussed earlier, many regulatory steps leading to the translocation of NF- κ B involves ubiquitination of RIP1 and therefore RNF126 knockdown possibly prolongs RIP1 polyubiquitination and thereby NF- κ B activity, leading to the “no oscillation” phenotype by up-regulation of A20 as well as I κ B α (Fig. 5 A and 6). To determine whether the elevated I κ B α and A20 expression is indeed caused by enhanced NF- κ B activity before TNF α stimulation, the basal transcriptional activation of NF- κ B should be addressed during the pre-stimulation knockdown period.

Similar to PHF5A described earlier, cyclin dependent kinases such as CDK12 have been implicated in the processing of pre-mRNA (33). Although not yet described, knockdown of CDK12 could have a similar effect on the processing of I κ B α pre-mRNA as suggested for PHF5A above, resulting in the “delayed” phenotype (Fig. 2 A), and delayed re-expression of I κ B α protein (Fig. 5 A). The delay of I κ B α pre-mRNA processing and thus prolonged nuclear p65 presence would also explain the enhanced expression of A20.

TRIM8 is an E3 ubiquitin ligase that has been reported to activate the NF- κ B pathway by ubiquitinating the activating kinase TAK1 (34) as well as SOCS-1, a negative regulator of transcriptionally active NF- κ B (35,36). Reduction of TRIM8 thereby resulted in a non-responsive, “no oscillation” phenotype with basic enhanced levels of A20 protein (Fig. 6). Of all candidate gene knockdowns leading to the “no oscillation” phenotype, the effect of TRIM8 knockdown seems to rely most on A20 upregulation as double knockdown for TRIM8 and A20 completely restored and even increased the NF- κ B oscillatory response (Fig. 7).

In summary, using an advanced systems microscopy approach involving high content imaging and RNA interference screening, we identified novel regulators of NF- κ B signaling. Some of these regulators were essential to control the TNF α -dependent cell death by controlling the expression levels of A20, a negative feedback regulator of TNF receptor signaling. Besides in cytotoxicity, our candidate genes are likely to have important functions in inflammation and in the development or progression of different diseases including cancer, rheumatoid arthritis and pathogen infection. This needs further exploration.

ACKNOWLEDGEMENTS

This work was performed under the framework of the Dutch Top Institute Pharma project D3-201 and the Netherlands Toxicogenomics Center supported by the Netherlands Genomics Initiative.

REFERENCES

1. Hayden MS, West AP, Ghosh S. NF-kappaB and the immune response. *Oncogene* 2006;25:6758–6780.
2. Courtois G, Gilmore TD. Mutations in the NF-kappaB signaling pathway: implications for human disease. *Oncogene* 2006;25:6831–6843.
3. Karin M, Lin A. NF-kappaB at the crossroads of life and death. *Nat Immunol* 2002;3:221–227.
4. Shen H-M, Tergaonkar V. NFkappaB signaling in carcinogenesis and as a potential molecular target for cancer therapy. *Apoptosis* 2009;14:348–363.
5. Fredriksson L, Herpers B, Benedetti G, Matadin Q, Puigvert JC, de Bont H, et al. Diclofenac inhibits tumor necrosis factor- α -induced nuclear factor- κ B activation causing synergistic hepatocyte apoptosis. *Hepatology* 2011;53:2027–2041.
6. Zhang L, Jiang G, Yao F, He Y, Liang G, Zhang Y, et al. Growth inhibition and apoptosis induced by osthole, a natural coumarin, in hepatocellular carcinoma. *PLoS ONE* 2012;7:e37865.
7. Israël A. The IKK complex, a central regulator of NF-kappaB activation. *Cold Spring Harb Perspect Biol* 2010;2:a000158.
8. Hayden MS, Ghosh S. Shared principles in NF-kappaB signaling. *Cell* 2008;132:344–362.
9. Staudt LM. Oncogenic activation of NF-kappaB. *Cold Spring Harb Perspect Biol* 2010;2:a000109.
10. Halsey TA, Yang L, Walker JR, Hogenesch JB, Thomas RS. A functional map of NFkappaB signaling identifies novel modulators and multiple system controls. *Genome Biol* 2007;8:R104.
11. Chew J, Biswas S, Shreeram S, Humaidi M, Wong ET, Dhillon MK, et al. WIP1 phosphatase is a negative regulator of NF-kappaB signalling. *Nat Cell Biol* 2009;11:659–666.
12. Li S, Wang L, Berman MA, Zhang Y, Dorf ME. RNAi screen in mouse astrocytes identifies phosphatases that regulate NF-kappaB signaling. *Mol Cell* 2006;24:497–509.
13. Ashall L, Horton CA, Nelson DE, Paszek P, Harper CV, Sillitoe K, et al. Pulsatile stimulation determines timing and specificity of NF-kappaB-dependent transcription. *Science* 2009;324:242–246.
14. Tian B, Nowak DE, Brasier AR. A TNF-induced gene expression program under oscillatory NF-kappaB control. *BMC Genomics* 2005;6:137.
15. Nelson DE, Ihekweba AEC, Elliott M, Johnson JR, Gibney CA, Foreman BE, et al. Oscillations in NF-kappaB signaling control the dynamics of gene expression. *Science* 2004;306:704–708.
16. Perkins ND. Post-translational modifications regulating the activity and function of the nuclear factor kappa B pathway. *Oncogene* 2006;25:6717–6730.
17. Iwai K. Diverse ubiquitin signaling in NF- κ B activation. *Trends Cell Biol* 2012;22:355–364.
18. Wajant H, Scheurich P. TNFR1-induced activation of the classical NF- κ B pathway. *FEBS J* 2011;278:862–876.
19. Werner SL, Kearns JD, Zadorozhnyaya V, Lynch C, O'Dea E, Boldin MP, et al. Encoding NF-kappaB temporal control in response to TNF: distinct roles for the negative regulators I κ B α and A20. *Genes Dev* 2008;22:2093–2101.
20. Puigvert JC, de Bont H, van de Water B, Danen EHJ. High-throughput live cell imaging of apoptosis. *Curr Protoc Cell Biol* 2010;Chapter 18:Unit 18.10.1–13.
21. Poser I, Sarov M, Hutchins JRA, Hériché J-K, Toyoda Y, Pozniakovskiy A, et al. BAC TransgeneOmics: a high-throughput method for exploration of protein function in mammals. *Nat Methods* 2008;5:409–415.
22. Hendriks G, Atallah M, Morolli B, Calléja F, Ras-Verloop N, Huijskens I, et al. The ToxTracker assay: novel GFP reporter systems that provide mechanistic insight into the genotoxic properties of chemicals. *Toxicol Sci* 2012;125:285–298.
23. Takami Y, Nakagami H, Morishita R, Katsuya T, Cui T-X, Ichikawa T, et al. Ubiquitin carboxyl-terminal hydrolase L1, a novel deubiquitinating enzyme in the vasculature, attenuates NF-kappaB activation. *Arterioscler Thromb Vasc Biol* 2007;27:2184–2190.
24. Tan P, Fuchs SY, Chen A, Wu K, Gomez C, Ronai Z, et al. Recruitment of a ROC1-CUL1 ubiquitin ligase by Skp1 and HOS to catalyze the ubiquitination of I κ B α . *Mol Cell* 1999;3:527–533.
25. Gorska MM, Liang Q, Stafford SJ, Goplen N, Dharajiya N, Guo L, et al. MK2 controls the level of negative feedback in the NF-kappaB pathway and is essential for vascular permeability and airway inflammation. *J Exp Med* 2007;204:1637–1652.
26. Rzymiski T, Grzmil P, Meinhardt A, Wolf S, Burfeind P. PHF5A represents a bridge protein between splicing proteins and ATP-dependent helicases and is differentially expressed during mouse spermatogenesis. *Cytogenet Genome Res* 2008;121:232–244.
27. Kant S, Schumacher S, Singh MK, Kispert A, Kotlyarov A, Gaestel M. Characterization of the atypical MAPK ERK4 and its activation of the MAPK-activated protein kinase MK5. *J Biol Chem* 2006;281:35511–35519.
28. Shiryayev A, Dumitriu G, Moens U. Distinct roles of MK2 and MK5 in cAMP/PKA- and stress/p38MAPK-induced heat shock protein 27 phosphorylation. *J Mol Signal* 2011;6:4.
29. Parcellier A, Schmitt E, Gurbuxani S, Seigneurin-Berny D, Pance A, Chantôme A, et al. HSP27

is a ubiquitin-binding protein involved in I-kappaB α proteasomal degradation. *Mol Cell Biol* 2003;23:5790–5802.

30. Park K-J, Gaynor RB, Kwak YT. Heat shock protein 27 association with the I kappa B kinase complex regulates tumor necrosis factor alpha-induced NF-kappa B activation. *J Biol Chem* 2003;278:35272–35278.
31. Jin Z, Li Y, Pitti R, Lawrence D, Pham VC, Lill JR, et al. Cullin3-based polyubiquitination and p62-dependent aggregation of caspase-8 mediate extrinsic apoptosis signaling. *Cell* 2009;137:721–735.
32. Bays NW, Hampton RY. Cdc48-Ufd1-Npl4: stuck in the middle with Ub. *Curr Biol* 2002;12:R366–71.
33. Loyer P, Trembley JH, Katona R, Kidd VJ, Lahti JM. Role of CDK/cyclin complexes in transcription and RNA splicing. *Cell Signal* 2005;17:1033–1051.
34. Li Q, Yan J, Mao A-P, Li C, Ran Y, Shu H-B, et al. Tripartite motif 8 (TRIM8) modulates TNF α - and IL-1 β -triggered NF- κ B activation by targeting TAK1 for K63-linked polyubiquitination. *Proc Natl Acad Sci U S A* 2011;108:19341–19346.
35. Toniato E, Chen XP, Losman J, Flati V, Donahue L, Rothman P. TRIM8/GERP RING finger protein interacts with SOCS-1. *J Biol Chem* 2002;277:37315–37322.
36. Strebovsky J, Walker P, Lang R, Dalpke AH. Suppressor of cytokine signaling 1 (SOCS1) limits NFkappaB signaling by decreasing p65 stability within the cell nucleus. *FASEB J* 2011;25:863–874.

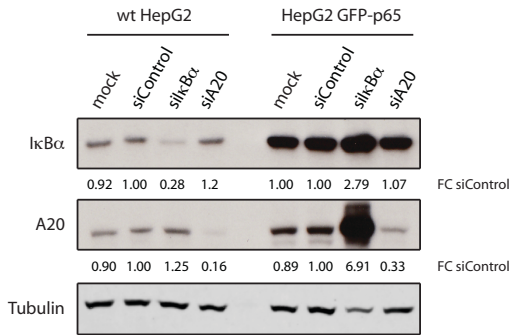
References in Table 1

1. Takami Y, Nakagami H, Morishita R, Katsuya T, Cui T-X, Ichikawa T, et al. Ubiquitin carboxyl-terminal hydrolase L1, a novel deubiquitinating enzyme in the vasculature, attenuates NF-kappaB activation. *Arterioscler Thromb Vasc Biol* 2007;27:2184–2190.
2. Rompe F, Artuc M, Hallberg A, Alterman M, Stroder K, Thone-Reineke C, et al. Direct angiotensin II type 2 receptor stimulation acts anti-inflammatory through epoxyeicosatrienoic acid and inhibition of nuclear factor kappaB. *Hypertension* 2010;55:924–931.
3. Guo R-W, Yang L-X, Wang H, Liu B, Wang L. Angiotensin II induces matrix metalloproteinase-9 expression via a nuclear factor-kappaB-dependent pathway in vascular smooth muscle cells. *Regul Pept* 2008;147:37–44.
4. Gorska MM, Liang Q, Stafford SJ, Goplen N, Dharajiyi N, Guo L, et al. MK2 controls the level of negative feedback in the NF-kappaB pathway and is essential for vascular permeability and airway inflammation. *J Exp Med* 2007;204:1637–1652.
5. Lee MH, Mabb AM, Gill GB, Yeh ETH, Miyamoto S. NF-kappaB induction of the SUMO protease SENP2: A negative feedback loop to attenuate cell survival response to genotoxic stress. *Mol Cell* 2011;43:180–191.
6. Fenner BJ, Scannell M, Prehn JHM. Expanding the substantial interactome of NEMO using protein microarrays. *PLoS ONE* 2010;5:e8799.
7. Shembade N, Harhaj EW. Regulation of NF-kappaB signaling by the A20 deubiquitinase. *Cell Mol Immunol* 2012;9:123–130.
8. Hayden MS, Ghosh S. NF- κ B, the first quarter-century: remarkable progress and outstanding questions. *Genes Dev* 2012;26:203–234.
9. Hatzoglou A, Roussel J, Bourgeade MF, Rogier E, Madry C, Inoue J, et al. TNF receptor family member BCMA (B cell maturation) associates with TNF receptor-associated factor (TRAF) 1, TRAF2, and TRAF3 and activates NF-kappa B, elk-1, c-Jun N-terminal kinase, and p38 mitogen-activated protein kinase. *J Immunol* 2000;165:1322–1330.
10. Alexaki V-I, Pelekanou V, Notas G, Venihaki M, Kampa M, Dessirier V, et al. B-cell maturation antigen (BCMA) activation exerts specific proinflammatory effects in normal human keratinocytes and is preferentially expressed in inflammatory skin pathologies. *Endocrinology* 2012;153:739–749.
11. Thu KL, Pikor LA, Chari R, Wilson IM, Macaulay CE, English JC, et al. Genetic disruption of KEAP1/CUL3 E3 ubiquitin ligase complex components is a key mechanism of NF-kappaB pathway activation in lung cancer. *J Thorac Oncol* 2011;6:1521–1529.
12. Lee D-F, Kuo H-P, Liu M, Chou C-K, Xia W, Du Y, et al. KEAP1 E3 ligase-mediated downregulation of NF-kappaB signaling by targeting IKKbeta. *Mol Cell* 2009;36:131–140.
13. Placke T, Kopp H-G, Salih HR. Glucocorticoid-induced TNFR-related (GITR) protein and its ligand in antitumor immunity: functional role and therapeutic modulation. *Clin Dev Immunol* 2010;2010:239083.
14. Tan P, Fuchs SY, Chen A, Wu K, Gomez C, Ronai Z, et al. Recruitment of a ROC1-CUL1 ubiquitin ligase by Skp1 and HOS to catalyze the ubiquitination of I kappa B alpha. *Mol Cell* 1999;3:527–533.
15. Suzuki H, Chiba T, Suzuki T, Fujita T, Ikenoue T, Omata M, et al. Homodimer of two F-box proteins betaTrCP1 or betaTrCP2 binds to I kappa B α for signal-dependent ubiquitination. *J Biol Chem* 2000;275:2877–2884.
16. Minoda Y, Sakurai H, Kobayashi T, Yoshimura A, Takaesu G. An F-box protein, FBXW5, negatively

regulates TAK1 MAP3K in the IL-1beta signaling pathway. *Biochem Biophys. Res Commun* 2009;381:412–417.

17. Israël A. The IKK complex, a central regulator of NF-kappaB activation. *Cold Spring Harb Perspect Biol* 2010;2:a000158.
18. Sun S-C. The noncanonical NF-kappaB pathway. *Immunol Rev* 2012;246:125–140.
19. Tan J, Kuang W, Jin Z, Jin F, Xu L, Yu Q, et al. Inhibition of NFkappaB by activated c-Jun NH2 terminal kinase 1 acts as a switch for C2C12 cell death under excessive stretch. *Apoptosis* 2009;14:764–770.
20. Zha J, Han K-J, Xu L-G, He W, Zhou Q, Chen D, et al. The Ret finger protein inhibits signaling mediated by the noncanonical and canonical IkappaB kinase family members. *J Immunol* 2006;176:1072–1080.
21. Li Q, Yan J, Mao A-P, Li C, Ran Y, Shu H-B, et al. Tripartite motif 8 (TRIM8) modulates TNF α - and IL-1 β -triggered NF- κ B activation by targeting TAK1 for K63-linked polyubiquitination. *Proc Natl Acad Sci U S A* 2011;108:19341–19346.
22. Toniato E, Chen XP, Losman J, Flati V, Donahue L, Rothman P. TRIM8/GERP RING finger protein interacts with SOCS-1. *J Biol Chem* 2002;277:37315–37322.
23. Strebovsky J, Walker P, Lang R, Dalpke AH. Suppressor of cytokine signaling 1 (SOCS1) limits NFkappaB signaling by decreasing p65 stability within the cell nucleus. *FASEB J* 2011;25:863–874.
24. Kovalenko A, Chable-Bessia C, Cantarella G, Israël A, Wallach D, Courtois G. The tumour suppressor CYLD negatively regulates NF-kappaB signalling by deubiquitination. *Nature* 2003;424:801–805.
25. Gewurz BE, Towfic F, Mar JC, Shinnars NP, Takasaki K, Zhao B, et al. Genome-wide siRNA screen for mediators of NF-kappaB activation. *Proc Natl Acad Sci U S A* 2012;109:2467–2472.
26. Li S, Zheng H, Mao A-P, Zhong B, Li Y, Liu Y, et al. Regulation of virus-triggered signaling by OTUB1- and OTUB2-mediated deubiquitination of TRAF3 and TRAF6. *J Biol Chem* 2010;285:4291–4297.
27. Komander D, Barford D. Structure of the A20 OTU domain and mechanistic insights into deubiquitination. *Biochem J* 2008;409:77–85.
28. Schweitzer K, Bozko PM, Dubiel W, Naumann M. CSN controls NF-kappaB by deubiquitinylation of IkappaBalpha. *EMBO J* 2007;26:1532–1541.

SUPPORTING DATA



Supporting Data S1. *siRNA-mediated knockdown is successful in wildtype and GFP-p65 HepG2 cells. 50 nM siRNA SMARTpool transfection on positive controls, siA20 and siIkBα results in successful knockdown using INTERFERIN transfection reagent, as determined by western blotting. In GFP-p65 cells the siIkBα results in higher IκBα levels after 72 hours of knockdown, since knockdown of this inhibitor leads to enhanced p65 activity during this period and thereby increased IκBα transcription.*

Supporting Data S2. *Expression of IκBα-GFP does not enhance the levels of the protein. Stable expression of BAC-IκBα-GFP does not result in overexpression of this protein. Furthermore, the GFP-tagged version of this protein behaves as the endogenous protein following TNFα (10 ng/mL) exposure, as determined by western blotting.*

